Journal of Academia and Industrial Research (JAIR)
Volume 10, Issue 3, Pages 39-49

ISSN: 2278-5213

Research Article

Self-driving Behaviors and Spontaneous Driving of Liquid Droplets on Micro-structured Graphene with Ultra-low Pinning Effect

Abubaker Abdelgalil Mohamed*
Department of Mechanical Engineering, Jiangsu University, Zhenjiang city, Jiangsu Province, 2077 Tower, China
abubakergalil@gmail.com* +971563541160
Received: February 21 2022/Accepted: April 26 2022/Published: 07 May 2022

Abstract

Recently, with the rapid development in the technology of micro-nano fluidics system and devices, micro-nano fluidics and self-driving droplets has attracted and received more and more attention in many scientific and engineering fields. In this Paper, the self-driving motion and behaviors of mercury droplets on the surface of the textured copper-graphene composite substrate have been explored, studied, and simulated by using the molecular dynamics method. Firstly, the composite substrate of the monolayered graphene with the trapezoidal grooves has been designed to study and understand the influence and behavior of the mercury droplets on the copper-graphene surface. The results from the experiment show that the mercury droplet can move spontaneously in the composite surface from a very narrow to a wide end of the groove on the trapezoidal surface due to the changes in the interacting potential energy between the droplet and substrate. Secondly, the energy method was used to calculate the total energy of the system as the droplet was adsorbed on the surface of the rectangular groove, and the self-driving mechanism of the droplet on the surface of the trapezoidal groove was also studied. Finally, The reduction of pinning effect by mono-layer graphene surface by making mercury droplet moves uniformly with constant slow velocity across different defects has been compared and studied between grapheme-covered Cu and pure Cu substrate with the considering the size effect and structuring parameter of the defect to obtain the reduction of pinning effect by mono-layer graphene. The interfacial energy and the force versus the displacement have been calculated and analyzed by the surface tension theory. The results show that a mercury liquid or droplet can occur self-propagation spontaneously on a copper-graphene monolayer without inputting any external energy, and the molecular dynamics simulation reveals that the mercury droplet undergoes acceleration and deceleration from narrow to wide ends of the groove on the Cu substrate covered by the mono-layer graphene surface.

Keywords: Molecular dynamics simulation, copper, graphene; Mercury droplet, pinning effect, energy barrier.

Introduction

The motion behaviors of the droplet on the hydrophobic solid surfaces have attracted considerable attention in recent years. Especially for the self-driven droplets on the gradient fictionalized solid surface. Research carried out over the past couple of decades has established that controlled propulsion of liquid droplets on a solid surface generates not only fascinating science but also promises viable applications in various heat transfer and microfluidic technologies (Daniel *et al.*, 2005). The philosophy underlying such propulsion is to break the wetting symmetry of a droplet on a surface, which has been made possible by harnessing gradients of surface energy, light, temperature, electric force, mechanical vibration, or their combinations.

In the late 1950s, Alder and Wainwright introduced the molecular dynamics method to study the interactions of hard spheres (Alder and Wainwright, 1957; Stillinger and Rahman, 1974). Many essential insights concerning the behavior of pure liquids emerged from their studies. Over the years, scientists and engineers have been fascinated by the directional transport of liquid droplets on a fictionalized surface and it has become a challenge for researchers in the field of nanotechnology and micro-fluidics. One of the preseasons that make the directional transport of liquid droplets important in recent years is that it does not require any energy supply and the self-driven droplet is a good example to study in this novel design.

*Corresponding author

Droplet transport is increasingly becoming popular for various micro-fluidic applications. In 1992, Chaudhury has obtain the up and downhill motion of the liquid droplet which have found that a surface having a spatial gradient in its surface free energy was capable of causing the drops of water placed on it to move uphill and the results show that a gradient of hydrophobic over a distance of 1 centimeter (Chaudhury *et al.,* 1992).

Water is the most abundant resource in nature. However, the portable water available for living organisms is rather confined, and the amount is constantly diminishing. On top of that, accessible fresh water is unevenly distributed over the surface of the earth. Water scarcity is more severe in arid areas, and living creatures in such areas must adapt to have special abilities to get water from atmospheric air for survival. The Namib Desert is one of the driest areas on the earth, and the only sustainable water resource is fog from the Atlantic Ocean. Thus, some living creatures in the Namib Desert adopt several strategies to collect water from the foggy air. In particular, several species among the Namib desert beetles have been reported to tilt their bodies toward the foggy wind to collect water droplets on their dorsal surfaces (Park and Kim, 2016; Fig. 1). In 1964 Rahman is the first to carry out a simulation using a realistic potential for liquid argon (Rahman *et al.,* 1694).

Fig. 1. Droplet transport in nature (Park and Kim, 2016).

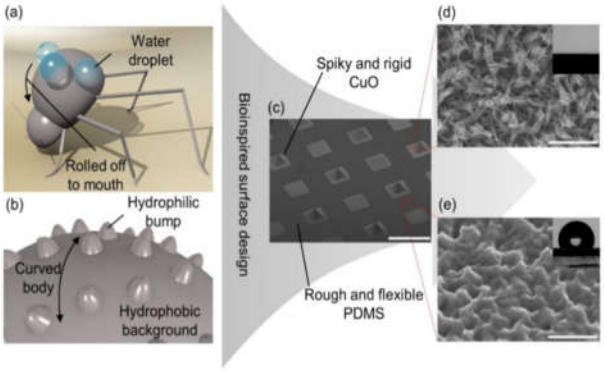

In 1974 Rahman and Stillinger is the first to do a molecular dynamics simulation of a practical system (Rahman and Stillinger, 1974). In 1947 Single-layer graphene was founded theoretically by P. R. Wallace. But first produced and identified in 2004, it is excellent mechanical, electrical, and thermal properties are amazing. Graphene Nano-channels have been found to achieve ultra-fast water transport (Haeberle *et al.,* 2008), which is mainly due to the considerable slip length on the surface, and the weak attraction of graphene and fluid is also a factor that causes rapid flow. Single-layer graphene has wetting and transparency (Shih and Strano, 2013).

The properties of the substrate will affect the wettability and movement behavior of the droplets on the surface of graphene, and the two-dimensional graphene film can only be used if it is transferred to the substrate. Therefore, studying the self-driven behavior of droplets on a substrate with a graphene coating will have important guiding significance for exploring efficient droplet driving. Microfluidics is widely used in the fields of biomedicine and chemistry because of their potential for small size, short analysis and diagnostic time, high sensitivity, and high productivity analysis (Park *et al.,* 2016). Recently, droplet-based microfluidic devices have received particular attention because unmixed oil or insulating droplets in the air may not contaminate and disperse each other (Fyen *et al.,* 2008). Several droplet-based applications have been demonstrated, including protein crystallization, polymerase chain reaction (PCR) (Chaudhury and Whitesides, 1992), kinase assays, and synthesis of molecules or nanoparticles. Microfluidics appeared in the early 1980s as a promising multidisciplinary technology, and since then Aroused great interest. Micro pesticides include the amount of liquid from microliters to picolitres and show many advantages such as fast mass and heat transfer, reduced use of reagents, and waste, the purpose of the detector can be reduced below nanometer, and the reaction time can be reduced to a few seconds. The reduction of assays or biological processes appears on the chip as an optimistic technique.

Graphene is a substance composed of pure carbon, with atoms arranged in a regular hexagonal pattern similar to graphite, but in a one-atom-thick sheet or flat monolayer of carbon atoms tightly packed into a two-dimensional honeycomb lattice or a single isolated layer of graphite. One of the very first patents about the production of graphene was filed in October 2002 entitled, "nano-scaled graphene plates", Two years later, in 2004 Andre Geim and Kostya Novoselov at the University of Manchester extracted single-atom-thick crystallites from bulk graphite. Geim and Novoselov received several awards for their pioneering research on graphene, notably Prize in physics (Geim and Morozov, 2004). Graphene is a 2-dimensional network of carbon atoms. These carbon atoms are bound within the plane by strong bonds into a honeycomb array comprised of six-membered rings. By stacking these layers on top of each other, the well-known 3-dimensional graphite crystal is formed. It is a fundamental building block for graphitic materials of all other dimensionalities, it can be wrapped up into 0D fullerenes, rolled into 1D nanotubes, or stacked into 3D graphite. Thus, graphene is nothing else than a single graphite layer. Graphene is chemically the most reactive form of carbon. The only type of carbon (and generally all solid materials) in which every single atom is in exposure to a chemical reaction from two sides (due to the 2D structure), Carbon atoms at the edge of graphene sheets

*Corresponding author

have chemical reactivity Graphene burns at shallow temperature (e.g., 350°C) and has the highest ratio of edgy carbons (in comparison with similar materials such as carbon nanotubes) (Morozov and Novoselov, 2008). The electronic properties of graphene are a zero-overlap semimetal (with both holes and electrons as charge carriers) with very high electrical conductivity (Kim and Zhao *et al.,* 2009). Electrons can flow through graphene more quickly than through even copper. The particles travel through the graphene sheet as if they carry on mass, as fast as just one hundredth that of the speed of light. High charge carrier mobility, for which values of 10,000 cm^2/Vs, in some cases, even 200,000 cm^2/Vs were reported (Geim *et al.,* 2009). In an insulator or semiconductor, an electron bound to an atom can break free only if it gets enough energy from heat or passing photon to jump the 'band gap' (Drexler and Eric, 1986). But in graphene, the gap is negligible. This is the main reason why graphene's electrons can move quickly and very fast. To calculate the strength of graphene, scientists used a technique called Atomic Force Microscopy. It was found that graphene is harder than diamond and about 300 times harder than steel. The tensile strength of graphene exceeds 1 TPa. It is stretchable up to 20% of its initial length. Graphene is a perfect thermal conductor Its thermal conductivity is much higher than all the other carbon structures such as carbon nanotubes, graphite, and diamond (>5000 W/m/K) at room temperature Graphite, the 3D version of graphene, shows a thermal conductivity about 5 times smaller (1000 W/m/K). Graphene, despite it, is only one atom thick graphene that is still visible to the naked eye. Due to its unique electronic properties, it absorbs a high 2.3% of the light that passes through it (Lee *et al.,* 2008). This one-atom-thick crystal can be seen with the naked eye (Krishnamurthy and Gadhamshetty, 2013).

Fig. 2. Study of self-driven droplets by Marangoni effect (Li *et al.,* 2016).

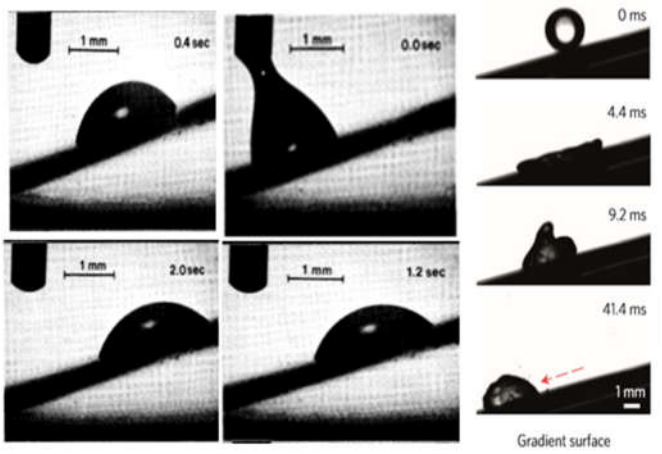

If the surface tension were to vary along with an interface, there would be an imbalance of force which in turn would cause flow. This flow is called the Marangoni effect, Surface tension depends on temperature and concentration of surfactant and so one way to create flow is to generate temperature or concentration changes (Fig. 2). In the 1860s, the Italian physicist Carlo Giuseppe is the first to describe the Marangoni effect which investigated the spreading of oil drops on a water surface. He explained this behavior as the macroscopic manifestation of liquid flow as a result of local differences (gradients) in interfacial tension. Many other examples of the expression of this phenomenon can be found in Refs (Fyen *et al.,* 2008). For liquids, the presence of even small amounts of foreign species can significantly reduce the surface tension. This is especially true for water that has an intrinsically high surface tension of 72.8 mN/m at room temperature. Because this value is significantly larger than for most other liquids (which are typically on the order of 20-40 mN/m), a large surface tension gradient exists due to a concentration gradient of foreign molecules at the water interface.

Materials and Methods

Experimental design: The Molecular Dynamics model designed in this research is composed of a copper substrate (Cu) with a gradient groove covered with a monolayer graphene single layer shown in Fig. 3.

Fig. 3. The MD model (a) and (b) for liquid mercury (Hg) droplet on a graphene-covered copper (Cu) substrate with a gradient structured groove.

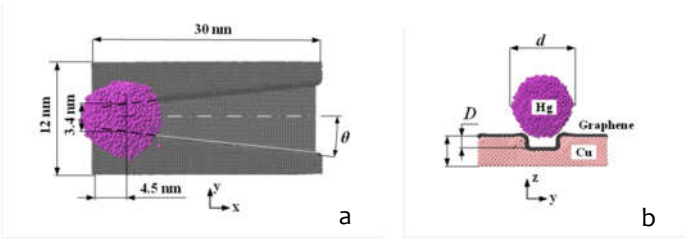

The green molecular cluster is the liquid Hg droplet, and the gray sheet is the graphene monolayer, which is covered on the pink grooved Cu substrate. The gradient width of the groove is characterized by an angle of θ, the depth of the groove is D while the diameter of the Hg droplet is d. The initial location of the Hg droplet is set to be 0. In this novel model, a single layer of graphene has been developed by Material Studio; the graphene length is 30 nm on the x-axis and 12 nm on the y-axis, and the graphene is placed on the top of a copper substrate with a trapezoidal groove. First, the absorption process has been made to put the single graphene layer on the top of the copper (Cu) substrate surface than the mercury droplet (Hg) under the same simulation system on top of the graphene coating surface,

*Corresponding author

and at the top of the narrow trapezoidal groove side, The initial droplet used contained 6848 mercury atoms. The diameter of the droplet after relaxation was about 6.4 nm. The movement process and self-driving mechanism of mercury droplets were studied, and the effects of different groove width gradients θ, groove depth D, and droplet diameter d on droplet movement were explored. For the simulation model, the mercury droplet size used in this study is 6.4 nm (6848 mercury atoms), 5 nm x 5 nm x 5 nm. The original form and the shape of the mercury droplet after relaxation.

The size of the simulation box is 280 × 150 × 130 Å3, and fixed boundary conditions are used in the three directions of x, y, and z. In the simulation process of droplet self-driving, the NVT ensemble is applied to the mercury droplets to control the temperature at 300 K. The LJ potential energy parameters between the atoms are shown in Table 1. The cutoff radius of the LJ interaction is set to 12 Å. The interaction between the mercury atoms in the droplet is approximately described by the proportional mercury potential in the form. The pairwise Lennard-Jones (LJ) potential $U_S^*(r) = U_S(\lambda r) = \sum_{j=3}^{9} a_{2j}^* r^{-2j}$ *the* formula is the initial Schwerdtfeger potential of mercury dimers, which is applied to match the density of liquid mercury at 300 K. the diameters are as follows, the groove width gradient θ is 8°, A droplet driving model with a groove depth D of 1.26 nm (7 layers of copper atoms thick), and a droplet diameter d of 6.4 nm.

Table 1. LJ potential energy parameters between Hg, C and Cu.

Atom *i*	Atom *j*	ε (eV)	σ (Å)
Hg	C	0.001267	3.321
Hg	Cu	0.007628	2.774
C	Cu	0.02758	3.083

The energy barrier at the junctions of the proposed zigzag model is the key issue to achieving unidirectional self-driving of Hg droplets because the solid edges at junctions will create a pinning effect on droplet movement. Here, we designed a novel model to study the energy barrier junction change and to achieve the pinning effect on the Hg droplet moving at a constant speed of 2.0 m/s, we designed three different types of structures with three different types of defects to study the influences on the mercury droplet moving in the constant speed mentioned above. At present, effective methods for driving droplets on solid surfaces mainly focus on droplet propulsion caused by gradient external fields (including temperature), mechanical vibration, electric force , light, and electric force and the self-driving force caused by the gradient surface energy stemming from the chemical gradient. The results will give a theoretical basis for the design of the graphene-covered textured surface to drive liquid droplets directional and spontaneously. In this junction model, a single layer of graphene has been developed by Material Studio; The graphene length is 20 nm on the x-axis, 20 nm on the y-axis, and 3 nm on the z-axis, the graphene is placed on the top of a copper substrate with a defect on the middle of the substrate. First, the absorption process has been made to put the single graphene layer on the top of the copper (Cu) substrate surface than the mercury droplet (Hg) under the same simulation system on top of the graphene coating surface, for a Hg droplet moving from x = 5 to 12 nm with a constant velocity of 2.0 m/s. The size of the junction model in the x and y directions are 20 × 20 nm^2, the initial droplet used contained 6848 mercury atoms. The diameter of the droplet after relaxation was about 6.4 nm. The movement process and self-driving mechanism of mercury droplets were studied, and the effects of different groove width gradients θ, groove depth D, and droplet diameter d on droplet movement were explored. The novel model is shown in Fig. 4.

Fig. 4. The novel model.

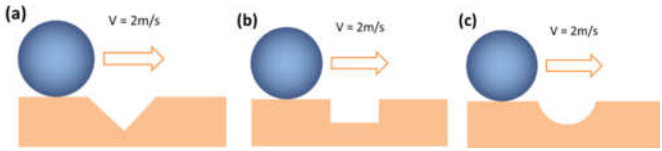

Fig. 4 shows the three different types of models with different defects, (a) Is the V shape defect model with the Hg droplet moving at a steady speed of 2 m/s, and (b) is the second defect type with the same speed and parameters, (c) is the U shape defect with the same parameters and speed as (a) and (b).

The pinning effect is a key issue to hinder the droplets from moving on the solid surface with defects. To investigate the reduction of the pinning effect by monolayer graphene and the corresponding mechanism, we make Hg and water droplets move uniformly (with a constant slow velocity (e.g. 2m/s) across different kinds of defects to calculate the interfacial energy/force, and potential energy of droplets themselves, etc. Compare the MD results between graphene-covered Cu and pure Cu substrates with considering the size effect and structuring parameters of defects. Finally, we can obtain the reduction of the pinning effect by monolayer graphene quantitatively from the calculation of the energy barrier from MD results. In this v shape junction model, we make the Hg droplet move across the junction with a slow constant velocity of 2.0 m/s to calculate the interfacial energy between droplets and substrates. graphene–Cu (G–Cu) junction model for a Hg droplet moving from x = 5 to 12 nm with a constant velocity of 2.0 m/s.

*Corresponding author

The size of the junction model in lateral x and y directions is 20 × 20 nm^2, where depth D = 1.08 nm and Hg diameter d = 6.4 nm.

Fig. 5 (a). Side view of the graphene–Cu (G–Cu) junction model for a Hg droplet moving from x = 5 to 12 nm with a constant velocity of 2.0 m/s. The size of the junction model in lateral x and y directions is 20 × 20 nm2, where D = 1.08 nm, (b) Is the top view for the v shape defect junction model.

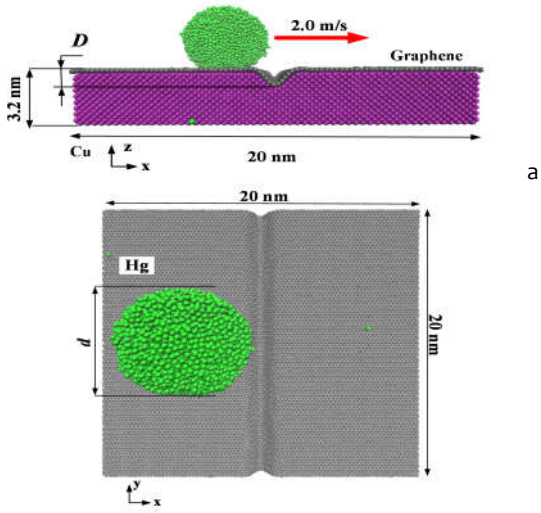

In this model, the diameters are as follows, A droplet driving model with a groove depth D of 1.08 nm (6 layers of copper atoms thick), and a droplet diameter d of 6.4 nm. Figure 5 shows the position of the droplet and its cross-sectional morphology at different times under this novel model. At t = 0 ns, the droplet starts moving at a steady speed of 2 m/s, At t = 2 ns, the droplet reached the area where the defect of 1.08 nm on a V shape is and starts the downhill, At t = 4 ns the droplet is already on the middle of the defect and starts the uphill process, At t = 6 ns the droplet moving on the substrate almost starts to relax and stop to finish the simulation process.

Fig. 6. The position and the cross-sectional v shape at the center of mass of the droplet at different times. Among them, the groove depth D is 1.08 nm, and the droplet diameter d is 6.4 nm. In the figure above, (a) (b) (c) and (d) represent the position and cross-section of the droplets at t = 0, 2, 4, and 6.0 ns, respectively.

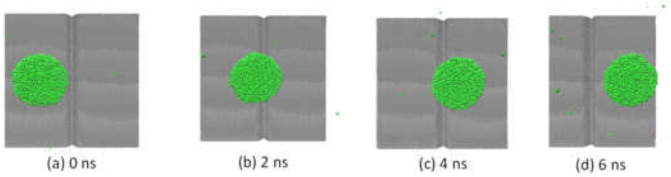

Results and Discussion

The movement of droplets on the surface of the grooved copper substrate without graphene coating was simulated. The shape parameters of the copper substrate are also θ = 7° and D = 1.26 nm, and Using droplets of the same size, the motion curve is shown below.

Fig. 7. The displacement (a) and velocity (b) of the droplet as a function of time on the surface of the grooves with graphene coating and without graphene coating.

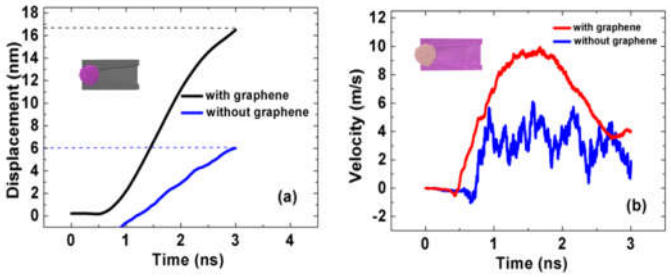

From the results graph above, it can be seen that the grooved substrate with graphene coating is more conducive to the self-driving of droplets. Its movement speed and maximum displacement are significantly higher than those without graphene coating, and the displacement and velocity curve of droplets is Smooth, indicating that the unidirectional movement trend of the droplet is more prominent. It's because of the smoothness of the graphene surface and the higher density of the surface, which makes the force of the droplet more uniform during the movement; and the adhesion between the droplet and graphene is smaller than that of copper, making it on the surface of the graphene coating less viscous resistance. Therefore, we believe that under the groove model proposed in this paper, graphene can significantly improve the self-driving effect of droplets. In the following simulations, the composite substrate with graphene coating was used, and the situation of driving droplets on the bare copper substrate was no longer considered. In this part of the study of the novel model discussed in the last part now Composite substrates with different groove width gradients, θ were constructed, and the values of θ were selected as 2 °, 4 °, 6 °, 8 °, and 11 °. At the same time, keep the size of the mercury droplet unchanged (droplet diameter is 5.8 nm), and the initial position of the mercury droplet remains constant (the mercury droplet centroid distance from the left end is 4.5 nm). The length of the groove also remains unchanged (the length is 30 nm), and the groove width at the initial position of the mercury is 3.4 nm. From the graphs shown below, the results show that the displacement and velocity curves of the droplet at different θ values that as the θ value increases, the maximum droplet displacement decreases.

*Corresponding author

Fig. 8. The displacement (a) and velocity (b) of droplets as a function of time under different groove width gradients. The groove depth D is 1.28 nm, the droplet diameter d is 6.4 nm, and the groove width gradients are 3 °, 4°, 6°, 8°, and 10°, respectively.

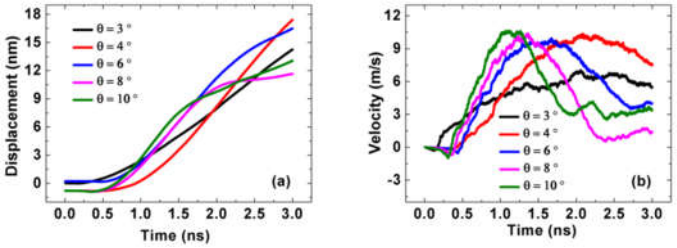

Composite substrates with different groove depths were constructed with groove depth D of 0.72, 0.90, 1.08, 1.26, and 1.44 nm (corresponding to the thickness of 4, 5, 6, 7, and 8 copper atoms, respectively). Keeping the groove width gradient unchanged (θ = 6°), the initial position of the mercury droplet remains unchanged, and the size of the mercury droplet remains the same. It can be seen from the droplet motion curve that is increasing the depth of the groove can increase the maximum displacement of the droplet (Fig. 9 left), and the acceleration and a maximum speed of the droplet increase with the depth of the groove (Fig. 10 right), which shows that increasing the thickness of the groove to a certain extent are conducive to droplet driving. The results below show the droplet velocity, and maximum displacement can be both increased by increasing the droplet size or by increasing the groove depth.

Fig. 9. The displacement(a) and velocity(b) of droplets as a function of time under different groove depths. Among them, the groove width gradient θ is 7°, and the droplet diameter d is 5.8 nm. The groove depths D of the substrate are 0.72, 0.90, 1.08, 1.26, and 1.44 nm, respectively.

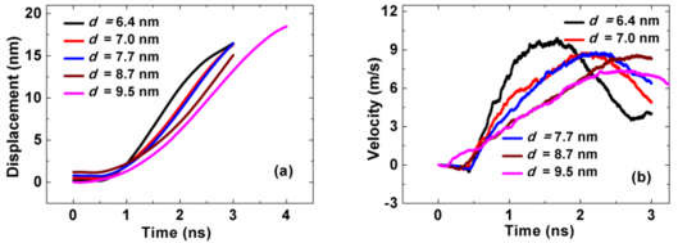

A composite substrate with θ = 6 ° and D = 1.26 nm was constructed. The initial position of the mercury droplets was unchanged, and the diameter d of the mercury droplets selected for relaxation was 6.4, 7.0, 7.7, 8.7, and 9.5 nm. By comparing the droplet motion curves under these five sizes (Fig. 9), it is found that on the same composite substrate surface, as the droplet size increases, the maximum displacement of the droplet motion increases, but its acceleration gradually decreases. Because the more significant the size, the smaller the specific surface area of the droplet, the effect of the interface between the droplet and the substrate on the movement of the droplet is reduced, and the phenomenon that the acceleration of the droplet decreases as the size of the droplet increases.

Fig. 10. The displacement(a) and velocity(b) of droplets as a function of time under different droplet sizes. Among them, the groove width gradient θ is 7 °, the groove depth D is 1.26 nm, and the droplet diameters d are 6.4, 7.0, 7.7, 8.7, and 9.5 nm, respectively.

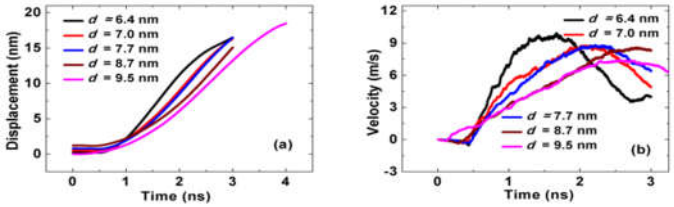

To explore the mechanism of driving the droplet on the surface of the groove, firstly, the change of the force Fx in the x-direction received by the droplet during the movement is counted, as shown in Fig. 10. It can be seen that initially Fx gradually decreases with the movement of the droplet in the x-direction, and decreases to zero around t = 1.04 ns, then the Fx transition direction becomes negative, and the value gradually increases, which causes the droplet speed to increase first and decreases which reach a maximum at t = 1.04 ns. At the same time, the interaction energy between the droplet and the copper-graphene composite substrate and the change in the potential energy of the droplet itself is counted.

Fig. 11(a). The force in x-direction Fx and the velocity of Hg droplet as functions of time. (b) The interfacial interaction energy between Hg droplet and Cu-graphene substrate versus time and the potential energy of Hg droplet versus time. EHg-Cu is the interaction energy between the Hg droplet and Cu substrate, EHg-C is the interaction energy between the Hg droplet and the graphene monolayer, EHg-sub is the interaction energy between the Hg droplet and the Cu-graphene composite substrate, EHg is the potential energy of Hg droplet. The width gradient θ = 6°, the groove depth D = 1.26 nm, and the droplet diameter d = 6.4 nm.

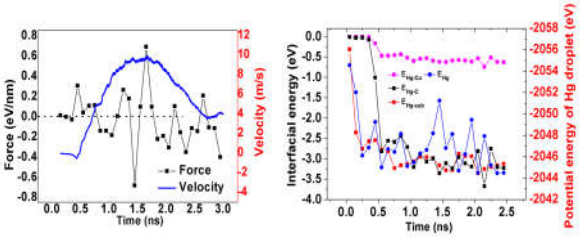

*Corresponding author

Continuing the study on the typical model shown in the previous chapter we no use the same model but with a double graphene layer to study the differences and influences on the mercury droplet moving on single, double, and triple graphene layers using the same droplet size and the same groove gradient size, the results are as shown that for the droplet velocity on double and triple the droplet moves to high speed faster compared to the one layer graphene-coated surface and throughout the process the more number of graphene layers the less velocity. Figure 12 shows the displacement study on different numbers of graphene layers and the results also confirm that the greater number of the graphene layers coated on the surface the higher the acceleration for the velocity and displacement.

Fig. 12. The displacement(a) and velocity(b) of droplets as a function of time under different droplet sizes. Among them, the groove width gradient θ is 6°, the groove depth D is 1.26 nm, and the droplet diameters d are 6.4 on a different number of graphene layers.

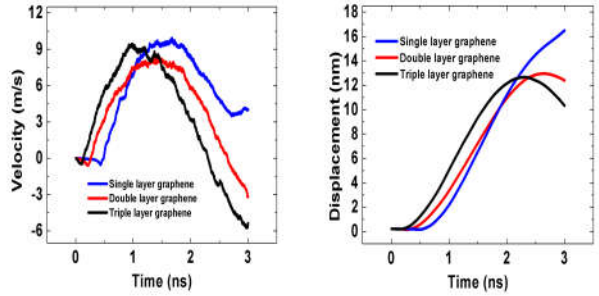

To explore the mechanism of driving the droplet on the surface of the groove, firstly, the change of the energy E(v) in the x-direction received by the droplet on different graphene layers number, as shown in Fig. 13 (a) It can be seen that initially the energy decrease with the increase of the graphene layers number for EHg-C, Fig. 13 (b) It can be seen that initially the energy increase with the increase of the graphene layers number for EHg-Cu.

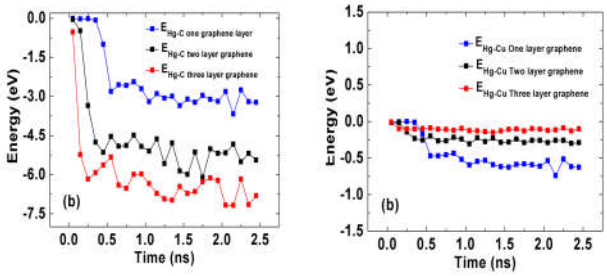

Fig. 13 (a) The force in x-direction Fx and the velocity of Hg droplet as functions of time on different numbers of graphene layers. (b) The interfacial interaction energy between Hg droplet and Cu-graphene substrate versus time and the potential energy of Hg droplet versus time. EHg-Cu is the interaction energy between Hg droplets and Cu substrate, EHg-C is the interaction energy between Hg droplets and the graphene monolayer, EHg-sub is the interaction energy between Hg droplets and the Cu-graphene composite substrate, EHg is the potential energy of Hg droplet. The width gradient θ = 6°, the groove depth D = 1.26 nm, and the droplet diameter d = 6.4 nm. It can be seen from Fig. 13 that the interfacial energy versus the displacement of the Hg droplet for both the graphene–Cu and pure Cu substrates. From the graph below, a clear energy peak can be observed concerning the drop of mercury moving across the pure copper intersection while very small energy fluctuations appear at the junction of the copper-graphene model. It proves that the graphene monolayer can highly reduce the pinning effect on the mercury droplet as shown in the results of the graph in Fig. 14.

Fig. 14. Comparing the interfacial energy between G–Cu and pure Cu substrates as a function of displacement of the Hg droplet.

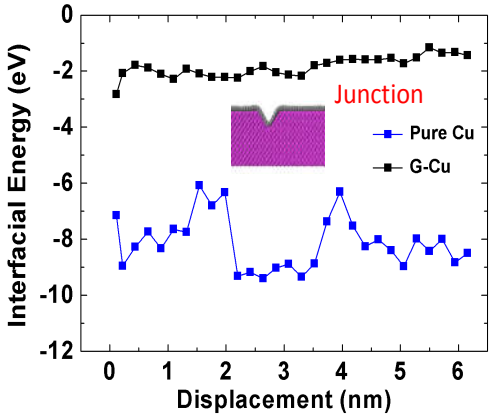

It can be seen from the displacement comparison below in Fig. 15 that comparing the copper with graphene monolayer with the one without the graphene (pure Cu) shows a small drop in the displacement compared to the G-Cu substrate. And this model can achieve continuous driving of droplets. The graphene coating increases the distance between the copper substrate and the droplets.

*Corresponding author

Figure 15 (a). The displacement results in the x-direction in the G-Cu substrate and the pure Cu substrate as a function of time.

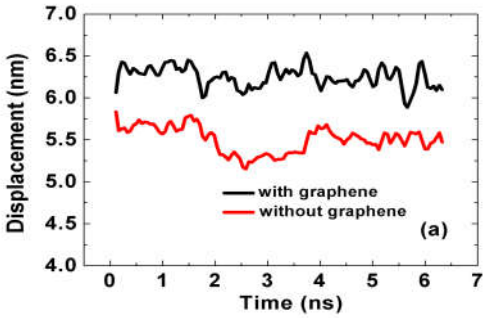

At the same time, the interaction energy between the droplet and the copper-graphene composite substrate and the change in the potential energy of the droplet itself is counted, as shown in Fig. 16. The interfacial interaction energy between Hg droplet and Cu-graphene substrate versus time. EHg-Cu is the interaction energy between the Hg droplet and Cu substrate, and EHg-C is the interaction energy between the Hg droplet and the graphene monolayer.

Fig. 16. The interfacial interaction energy between Hg droplet and Cu-graphene substrate versus time.

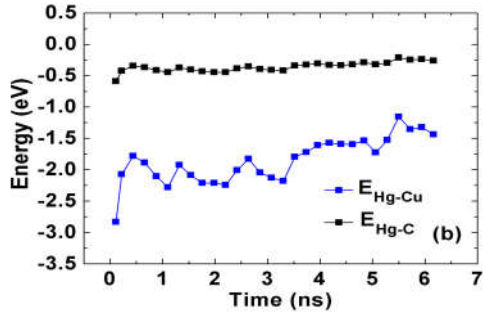

When studying the droplet movement and the molecular dynamics method is so important to do a comparison with different parameters to obtain the influences on different types of sizes so we get a brief understanding of the mechanism of the structure. Keeping the defect width gradient unchanged, the initial position of the mercury droplet remains unchanged, and the size of the mercury droplet remains the same. It can be seen from Fig. 16 that when comparing the same junction model with a different depth parameter d = 1.26 nm as a function of time (ns) it shows no big different curve as the depth of D = 1.08 compared to the self-driven droplet model, the Hg droplet size is still the same as d = 6.4 nm and on the same simulation conditions. Therefore, can obtain that the depth parameters do not influence the droplet displacement that much.

Fig. 17. Comparison between different depths parameters as a function of time with Hg droplet size still the same as in the typical model.

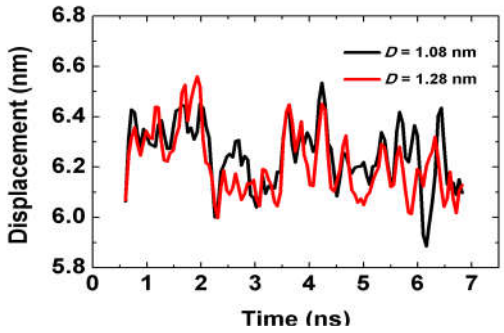

In this U shape junction model, by making the Hg droplet moves across the junction with a slow constant velocity of 2.0 m/s to calculate the interfacial energy between droplet and substrates. graphene–Cu (G–Cu) junction model for a Hg droplet moving from x = 5 to 12 nm with a constant velocity of 2.0 m/s. The size of the junction model in lateral x and y directions is 20 × 20 nm2, where depth D = 1.08 nm and Hg diameter d = 6.4nm. The parameters are the same as the v shape junction model.

Fig. 18. (a) Side view of graphene–Cu (G–Cu) junction u defect shape model for a Hg droplet moving from x = 5 to 12 nm with a constant velocity of 2.0 m/s. The size of the junction model in lateral x and y directions is 20 × 20 nm2, where D = 1.08 nm, (b) is the top view for u shape defect junction model.

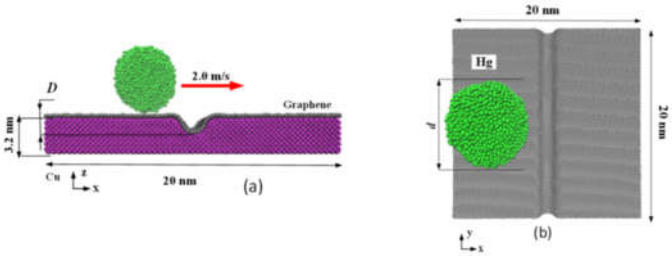

Fig. 19. The position and the cross-sectional v shape at the center of mass of the droplet at different times. Among them, the groove depth D is 1.08 nm, and the droplet diameter d is 6.4 nm. In the figure, (a) (b) (c) and (d) represent the position and cross-section of the droplets at t = 0, 2, 4, and 6.0 ns, respectively.

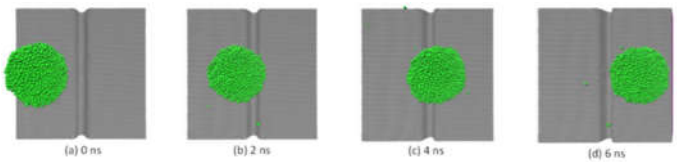

*Corresponding author

It can be seen from Fig. 19 for the u shape defect model that the interfacial energy versus the displacement of the Hg droplet for both the graphene–Cu and pure Cu substrates. From the graph below, a clear or huge energy peak can be observed concerning the drop of mercury moving across the pure copper intersection while very small energy fluctuations appear at the junction of the copper-graphene model. It proves that the graphene monolayer can significantly reduce the pinning effect on the mercury droplet as shown in the results of the graph in Fig. 20. Displacement 2 to 4 shows the time that the droplet moving at the slow speed of 2 m/s moves through the defect in the middle of the Cu substrate.

Fig. 20. Comparing the interfacial energy between G–Cu and pure Cu substrates as a function of displacement of the Hg droplet.

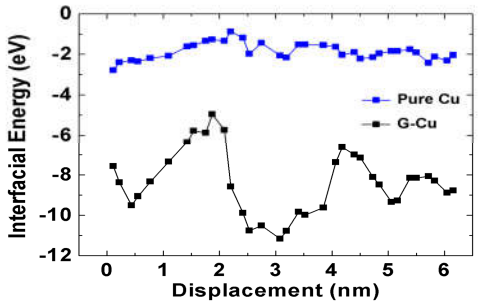

It can also be seen from the displacement comparison below in Fig. 21 that comparing the copper with graphene monolayer with the one without the graphene (Pure Cu) in u shape defect model shows a significant drop in the displacement compared to the G-Cu substrate as a function of time that the displacement becomes very low in the pure Cu substrate compared to the graphene monolayer Cu coating substrate.

Fig. 21. The displacement results in the x-direction in the G-Cu substrate and the pure Cu substrate as a function of time.

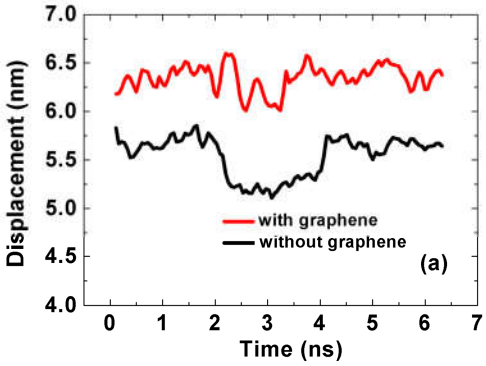

It can be seen from Fig. 22 that when comparing the same junction model with different depth parameters d = 1.26 nm as a function of time (ns) it shows no significant difference in the curve as the depth of D = 1.08 compared to the self-driven droplet model, the Hg droplet size is still the same as d = 6.4 nm and on the same simulation conditions. Nearly the same as the v shape defect results.

Fig. 22. Comparison between different depths parameters as a function of time with Hg droplet size still the same as in u shape defect model.

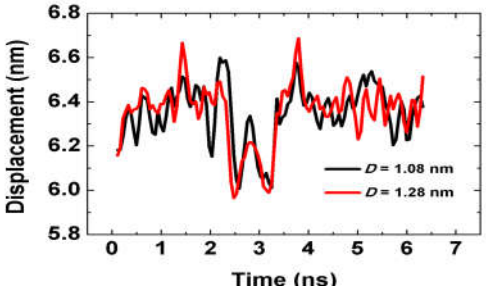

Figure 23 shows a comparison between the three different types of defect shape, it can be seen that for u shape defect the interfacial energy is significantly higher than the other and It is clear that from time 3 ns the hg droplets start moving slowly on the defect where the interfacial drops. So we can assume that the pinning effect has a significant effect on the interfacial energy of the slow-moving droplet.

Fig. 23. Comparison between different defect shapes for the displacement and the interfacial energy for Graphene-Cu substrate as a function of displacement.

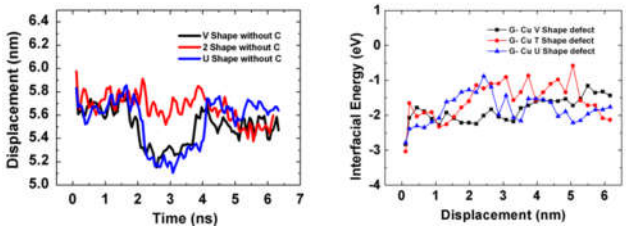

Fig. 24. Comparison between different defect shapes for the displacement and the interfacial energy for pure Cu substrate as a function of displacement.

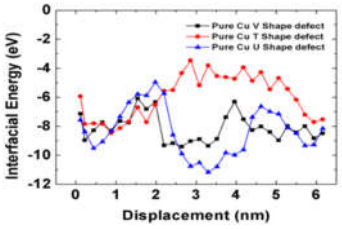

*Corresponding author

Conclusion

In this paper, the self-driving phenomenon of droplets on the surface of the copper texture-graphene composite substrate was simulated by the molecular dynamics method. Some texture models that can realize self-driving of droplets were proposed. Effect, and explored its self-driven mechanism. The main conclusions are as follows: Compared with the graphene-free copper substrate, the surface of the trapezoidal groove with graphene coating can significantly improve the self-driving effect of droplets. This is mainly because graphene has a certain liquid repellency and its surface is smoother so that the droplets are even during the movement. The droplets adsorbed on the narrow mouth end can spontaneously move to the wide mouth end, and the movement process is to accelerate first and then decelerate, and finally, the droplets will reciprocate or move away from the groove wall side for unidirectional movement, depending on the droplet acceleration and the maximum speed obtained. The movement speed of the droplet increases with the increase of the groove width gradient θ, but the maximum displacement decreases; to a certain extent, increasing the groove depth D will increase the droplet movement speed and maximum displacement, which can improve the droplet movement Effect, As the droplet size increases, the droplet movement speed will decrease, but its maximum displacement will increase. Initially, the energy decreases with the increase of the number of graphene layers number, and it can be seen that initially the energy increase with the increase of the number of graphene layers.

The effect of a single trapezoidal groove substrate on the movement of mercury droplet (Hg) on the surface of graphene coating copper substrate: First, the self-driving effect of mercury droplets on the surface of the trapezoidal groove substrate with and without graphene coating is compared. It is found that the droplets can move spontaneously from the narrow end to the wide end, but the graphene coating the layer can significantly increase the speed of the droplet movement. Then groove width of the different gradient and the groove depth affect droplet diameter droplet self-driven, all found in the model, movement droplets are accelerated and then decelerated, or from the final reciprocate The groove wall on one side moves unidirectionally (this depends on the maximum velocity obtained by the droplet); as the groove width gradient increases, the droplet velocity increases, but its maximum displacement decreases; and increases to a certain extent The depth of the groove can both increase the movement speed of the droplet and increase its maximum displacement; when the diameter of the droplet is gradually increased, the movement speed of the droplet decreases, but the maximum displacement increases. The pinning effect and interfacial energy of mercury droplets on a graphene monolayer Cu substrate have been studied by molecular dynamics simulation method and energy method. The research indicates that: a clear energy peak can be observed concerning the drop of mercury moving across the pure copper intersection while very small energy fluctuations appear at the junction of the copper-graphene model. It proves that the graphene monolayer can highly reduce the pinning effect on the mercury droplet as shown in the results. The graphene monolayer can significantly reduce the pinning effect on the self-driven droplet movement and process as shown in the results.

Acknowledgements

This work was supported by Jiangsu University (School of Mechanical Engineering Department).

References

1. Alder, B. J. and Wainwright, T. E. J. 1957. *Chem. Phys.* 27, 1208.
2. Balandin AA, Ghosh S, Bao W, et al. 2008. Superior thermal conductivity of single-layer graphene. *Nano Lett.* 8: 902–907.
3. Bormashenko, E. 2015. Self-propulsion of liquid marbles: Leidenfrost-like levitation driven by Marangoni flow. *J. Phys. Chem.* C 119: 9910–9915.
4. Brzoska, J. B., Brochard-Wyart, F. and Rondelez, F. 1993. Motions of droplets on hydrophobic model surfaces induced by thermal gradients. *Langmuir.* 9: 2220–2224.
5. Chaudhury, M. K. and Whitesides, G. M. 1992. How to make water run uphill. *Sci.* 256:1539–1541
6. Chaudhury,. M.K., Chakrabarti, A. and Daniel, S. 2015. Generation of motion of drops with inter facial contact. *Langmuir.*2-3.
7. Chu, K. H., Xiao, R. and Wang, E. N. 2010 Uni-directional liquid spreading on asymmetric nanostructured surfaces. *Na.Mater.* 9: 413–417.
8. Cira, N. J., Benusiglio, A. and Prakash, M. 2015. Vapour-mediated sensing, and motility in two-component droplets. *Nat.* 519: 446–450.
9. Dang W, Peng H, Li H, et al. 2010. Epitaxial Heterostructures of Ultrathin Topological Insulator Nanoplate and Graphene. *Nano Lett.* 10(8): 2870-2876.
10. Daniel, S., Chaudhury, M. K.and DeGennes, P. G. 2005. Vibration-actuated drop motion on surfaces for batch microfluidic processes. *Langmuir.* 21: 4240–4248.
11. Drexler, K. and Eric. 1986. Engines of Creation: The Coming Era of Nanotechnology. Double day. 0-385-19973-2.
12. Geim AK., Lee C1, Wei X, Kysar JW, Hone J. and prospects. 2009. Graphene. *Sci.* 324: 1530–1534.
13. Habenicht, A., Olapinski, M., Burmeister, F., Leiderer, P. and Boneberg, J. 2015. Jumping nano droplets. *Sci.* 309: 2043–2045.
14. Hua, J.L., Rouse, A. and Eckhardt, A.E. 2010. "Multiplexed real-time polymerase chain reaction on a digital microfluidic platform. *Analytical Chem.* 82(6): 2310–2316.

***Corresponding author**

15. Huebner, M., Srisa-Art, S. and Holt, D. 2007. Quantitative detection of protein expression in single cells using droplet microfluidics. *Chemical Commun.* 2(12): 1218–1220.
16. Ichimura, K., Oh, S.K. and Nakagawa, M. 2000. Light-driven motion of liquid sona photoresponsive surface. *Sci.* 288: 1624–1626.
17. Kim KS, Zhao Y, Jang H. 2009. Large-scale pattern growth of graphene films for stretchable transparent electrodes. *Nat.* 457: 706–710.
18. Krishnamurthy, A, Gadhamshetty, V. and Mukherjee, R. 2013. Passivation of microbial corrosion using a graphene coating. *Carbon*. 56:45-49.
19. Lee, C., Wei, X., Kysar, J.W. and Hone, J. 2008. Measurement of the elastic properties and intrinsic strength of monolayer grapheme. 18 (5887): 385-398.
20. Li, H. H. Pham, Z. Nie, B. MacDonald, A. Güenther, and E. Kumacheva. 2008. Multi-step microfluidic polymerization reactions conducted in droplets: the internal trigger approach. *J. Amer. Chem. Soc.* 130(30): 9935–9941.
21. McHale, G., Brown, C.V., Newton, M. I., Wells, G. G. and Sampara, N. 2011. Di electro wetting driven spreading of droplets. *Phys. Rev. Lett.*107, 186101.
22. Morozov SV, Novoselov KS, Katsnelson MI, et al. 2008. Giant intrinsic carrier mobilities in graphene and its bilayer. *Phys. Rev. Lett*. 100: 016602.
23. Neto, A Castro, Peres, N. M. R. Novoselov, K. S. Geim, A. K. Geim, A. K. 2009. The electronic properties of graphene. *Rev Mod Phys*. 81: 109–16.
24. Novoselov KS, Geim AK, Morozov SV. 2004. Electric field effect in atomically thin carbon films. Science. 306: 666–669.
25. Novoselov KS, Jiang D, Schedin F. 2005. Two-dimensional atomic crystals. *Proc Natl Acad Sci USA*. 102: 10451–10453.
26. Novoselov KS. Jiang D., Schedin F. and et al. 2005. Two-dimensional atomic crystals. *Proc Natl Acad Sci* USA. 102: 10451–10453.
27. Pollack, M. G., Fair, R. B. and Shenderov, A. D. 2000. Electrowetting-based actuation of liquid droplets for microfluidic applications. *Appl. Phys. Lett*. 77: 1725–1726.
28. Quéré, D. 2013. Leiden frost dynamics. Annu. Rev. Fluid Mech. 1-4.
29. Roach, H. Song, and R. F. Ismagilov. 2005. Controlling nonspecific protein adsorption in a plug-based microfluidic system by controlling interfacial chemistry using fluorous-phase surfactants. *Analyt. Chem*. 77(3): 785–796.
30. S. Haeberle, R. Zengerle. 2008. Microfluidic platforms for lab-on-a-chip applications.
31. S. Yadav. 2014. Graphene properties. Retrieved 29 May 2014. from http://www.graphene-battery.net. (In text: Yadav, 2014).
32. Shih C J, Strano M S, Blankschtein D. 2013. Wetting translucency of graphene. *Nature Materials*, 12(10): 866-869.
33. Song C L, Wang Y L, Jiang Y P, et al. 2010. Topological insulator Bi2Se3 thin films grown on double-layer graphene by molecular beam epitaxy. *Appl. Phy. Lett.* 97(14): 143118-143123.
34. Stillinger, F. H. and Rahman, A. J. 1974. Chem. Phys. 60, 1545.
35. Wang, K. Liu. and K. J. Chen et al., 2010. A rapid pathway toward a superb gene delivery system: programming structural and functional diversity into a supramolecular nanoparticle library. *ACS Nano*. 4(10): 6235–6243.
36. Wang, Z. et al., 2007. Polarity-dependent electrochemically controlled transport of water through carbon nanotube membranes. *Nano. Lett*. 7, 697–702.
37. Wang, Z.; Lin, K.; Zhao, Y.-P. 2019. The Effect of Sharp Solid Edges on the Droplet Wettability. *J. Colloid Interface Sci*. 552, 563–571.
38. Xian J, Li D, Chen J, et al. 2014. A large-area smooth graphene film on a TiO2 nanotube array via a one-step electrochemical process. *J. Mater. Chem*. 2(15): 5187-5192.
39. Zhao C, Deng B, Chen G. 2016. Large-area chemical vapor deposition-grown monolayer graphene-wrapped silver nanowires for broad-spectrum and robust antimicrobial coating. *Nano Res.* 9(4): 963-973.

Cite this Article as:

Abubaker, A.M. 2022. Self-driving behaviors and spontaneous driving of liquid droplets on micro-structured graphene with ultra-low pinning effect. *J. Acad. Indus. Res*. 10(3): 39-49.

***Corresponding author**